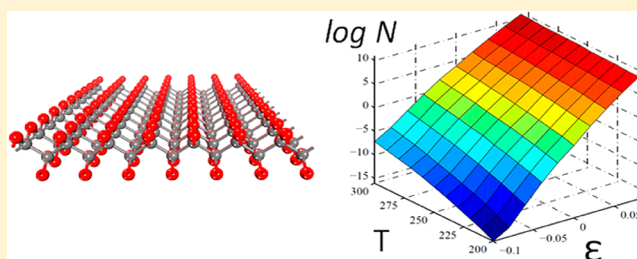


Structure, Stability, and Property Modulations of Stoichiometric Graphene Oxide

Shunhong Zhang,[†] Jian Zhou,[‡] Qian Wang,^{†,§,*} and Puru Jena[§][†]Center for Applied Physics and Technology, Peking University, Beijing 100871, China[‡]Department of Materials Science and Engineering, College of Engineering, Peking University, Beijing 100871[§]Department of Physics, Virginia Commonwealth University, Richmond, Virginia 23284, United States

Supporting Information

ABSTRACT: The recent success in synthesizing graphene monoxide (GMO) with rigorous stoichiometric ratio C:O = 1:1 has highlighted the need to determine its ground state geometry and to explore its physical properties. Using density functional theory and molecular dynamics simulation, we have found a new ether-type configuration of the GMO that is not only lower in energy than any other structures reported thus far, but is also stable up to 2000 K at which previous reported structures dissociate into CO molecules. The dynamic stability of the structure is further confirmed by calculating its phonon spectra. Furthermore, this ether-type structure exhibits anisotropies in mechanical stiffness and in electronic transport. Band gap, carrier concentration, and effective mass can be sensitively modulated by strain or higher oxidation level with C:O = 1:2. This study provides new theoretical insights into geometry, stability, and properties of the hotly pursued graphene oxide with unprecedented applications.



I. INTRODUCTION

The novel properties of graphene^{1,2} have recently caused a great deal of excitement in graphene-based materials research. One such example is graphene oxide (GO). Because of its solubility in water, ethanol, and other liquids, GO cannot only be used as a precursor for fabricating large-scale graphene but also allows the functionalization of the insoluble and infusible pristine graphene sheets, being flexibly tuned as an insulator, semiconductor, or semimetal with diverse possibilities for direct wiring with biomolecules, organic molecules, and other radical groups. However, one of the current challenges for practical application of GO is its structural characterization. Different experimental conditions, synthetic processes, oxygen-containing groups, and C:O ratio result in diverse geometries like amorphous phase with some locally ordered regions, ordered oxidized regions with some intact aromatic islands, and completely disordered phase. Current experimental methods such as ¹³C NMR,^{3,4} transmission electron microscopy (TEM), and X-ray diffraction^{5,6} can confirm the existence of certain functional groups but cannot provide detailed and accurate structure information.

Under such situations, GO systems with rigorous stoichiometric C:O ratio are highly desirable for better understanding GO-based materials. Recently, Mattson et al.⁷ have successfully synthesized graphene monoxide (labeled as GMO) through vacuum annealing of multilayered GO systems. They obtained an ordered nanocrystalline GMO structure with rigorous stoichiometric ratio of C:O = 1:1. This is the first report on the synthesis of GMO with such a high oxidation level, a

milestone by itself in GO research. In their article, the authors also suggested a possible GMO structure consisting of a quasi-hexagonal lattice with parallel-aligned epoxy pairs (labeled as ep-GMO). This structure is different from another structural model (labeled as mix-GMO) that was predicted theoretically⁸ before this synthesis. The ep-GMO was found to be 0.06 eV per formula unit higher in energy than the mix-GMO,⁸ where O exists in three configurations: normal epoxy, unzipped epoxy (ether group), and epoxy pair. Comparing the ep-GMO with the mix-GMO, we can expect that less number of epoxy pairs in the mix-GMO would result in the strain reduction, and hence would enhance its stability. Note that there is still no direct evidence for the ground state structure of the GMO. Thus, some important questions need to be addressed: (1) is there any other GMO configuration that is more stable both energetically and dynamically? (2) If so, is it possible to synthesize such a structure? (3) What novel properties will the new structure have, and how its properties can be further manipulated for potential applications? In this work, we carried out extensive studies to answer these questions. We have found a new structure that is more stable than any other structures reported thus far, and suggested possible precursors for the synthesis of this new structure. Moreover, the properties can be effectively manipulated by applying strain or oxidizing GMO to a higher level.

Received: November 4, 2012

Revised: December 20, 2012

Published: January 8, 2013

II. COMPUTATIONAL PROCEDURES

We carried out first principles calculations based on DFT by using a plane wave basis set and projected augmented waves (PAW)⁹ method implemented in the Vienna Ab initio Simulation Package (VASP).¹⁰ Exchange correlation functional is described by the Perdew-Burke-Ernzerhof (PBE) form within generalized gradient approximation (GGA) scheme.¹¹ The Monkhorst-Pack mesh¹² is adopted for Brillouin zone sampling. The kinetic energy cutoff is set at 500 eV. Geometric relaxations are performed by using conjugated gradient method with no symmetry constraints. The convergence criteria of total energy and Hellmann–Feynman force are set as 0.0001 eV and 0.01 eVÅ⁻¹, respectively. To simulate the 2D GMO, periodic boundary condition is applied and a vacuum layer of 15 Å is used along the normal direction of the basal plane of the GMO structure to avoid interactions between the GMO and its periodic images. To confirm its dynamic stability, phonon calculations are performed using finite displacement method as implemented in the phonopy program.¹³

III. RESULTS AND DISCUSSION

1. Structure and Stability. According to previous studies on the chemistry of GO and the oxidation mechanism of graphene, the ether-type configuration has been shown to be more stable than the epoxy-pair and the clamped epoxy type.^{14–16} The O-driven unzipping of clamped epoxide breaks the C network and gives rise to unzipped ether, and hence lowers the energy through release of local strain.^{14,15} Thus, we constructed a new GMO model by using the unzipped ether as the building block (Figure 1), which can be viewed as zigzag

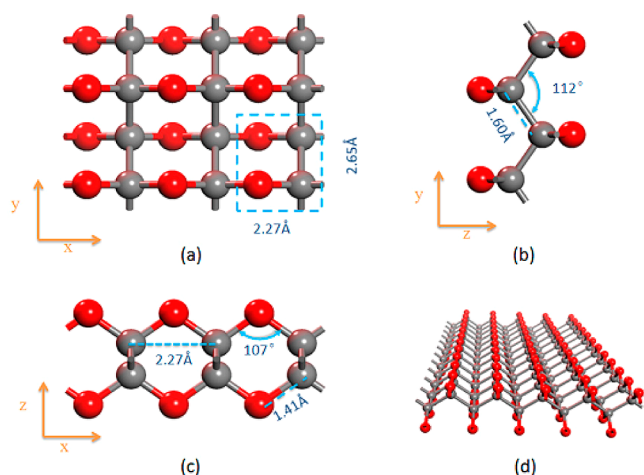


Figure 1. Different views of atomic structure of z-GMO along the z direction (a), the x direction (b), and the y direction (c). The perspective view is given in (d). The rectangle in (a) is for the unit cell. Gray and red (dark gray) balls are C and O atoms, respectively.

carbon chains linked by oxygen atoms, namely, having –C–O–C– zigzag chains in the x direction and –C–C–C– zigzag chains in the y direction. We label this structure as z-GMO. Note that all the C atoms are 4-fold coordinated having two bonds with its neighboring C atoms and two bonds with O atoms. After geometric relaxation, we found that the unit cell of the z-GMO becomes a rectangle with two lattice constants of 2.27 and 2.65 Å. The C–O bond length is 1.41 Å, which is comparable to that found in previous calculations.¹⁴ The relaxed C–C bond length is 1.60 Å, indicating a single σ bond

between them. The C–C–C angle is found to be 112°, slightly larger than that of the sp^3 hybridized C atoms, namely, 109°. The distance between the two C atoms linked by a bridging oxygen is 2.27 Å (part c of Figure 1), which is shorter than that in the unzipped ether groups¹⁴ (~2.50 Å) and longer than that in clamped epoxy¹⁴ (~1.50 Å) or epoxy pairs⁷ (1.92 Å).

Next we explore the stability of z-GMO model by examining its relative energy, phonon dispersion and thermal stability. First, we focus on the energetics of z-GMO, ep-GMO and mix-GMO structures (Figure 2). Detailed structural parameters can

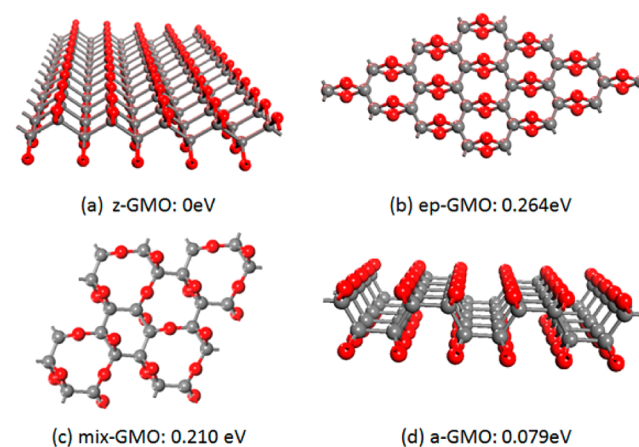


Figure 2. Structure and relative energy per formula unit (CO) of (a) z-GMO, (b) ep-GMO, (c) mix-GMO, and (d) a-GMO.

be found in the Supporting Information (SI). We found that the z-GMO model is lower in energy by 0.264 and 0.210 eV per formula unit (CO) than that of the ep-GMO and mix-GMO structures, respectively. Our calculated energy difference between the ep- and mix-GMO structures is 0.054 eV per formula unit in good agreement with previous study,⁸ confirming the accuracy of our calculations.

The stability of the z-GMO structure consisting of zigzag carbon chains inspired us to consider another possible structure composed of armchair carbon chains (labeled as a-GMO), as shown in part d of Figure 2. We found that it is 0.079 eV per formula unit higher in energy than the z-GMO structure, this can be attributed to two factors: the bonding angles in z-GMO are more close to sp^3 hybridization, and the O–O distance is longer by 0.013 Å, resulting in less Coulomb repulsion. But a-GMO is still 0.185 and 0.131 eV lower in energy than the ep- and mix-GMO structures, respectively. The underlying reasons for the low energy of z-GMO and a-GMO is that the ether-type configuration with C–O–C bonding reduces the local strain as compared to that of the epoxy-pair type in the ep- and mix-GMO.

From above we see that the z-GMO configuration is energetically much more stable than the two previously suggested structures. To examine its dynamical stability, we performed calculations of phonon spectra. The results are plotted in part a of Figure 3, where no imaginary frequencies exist, indicating that the z-GMO is dynamically stable. To further study its stability at finite-temperature, we performed ab initio molecular dynamics simulation at 300 K for 5000 steps with a time step of 1 fs using Nöse-Hoover heat bath¹⁵ scheme. To minimize the constraint induced by periodicity, a (3 × 3) supercell is used. The total energy variation with respect to simulation time is displayed in part b of Figure 3. The average

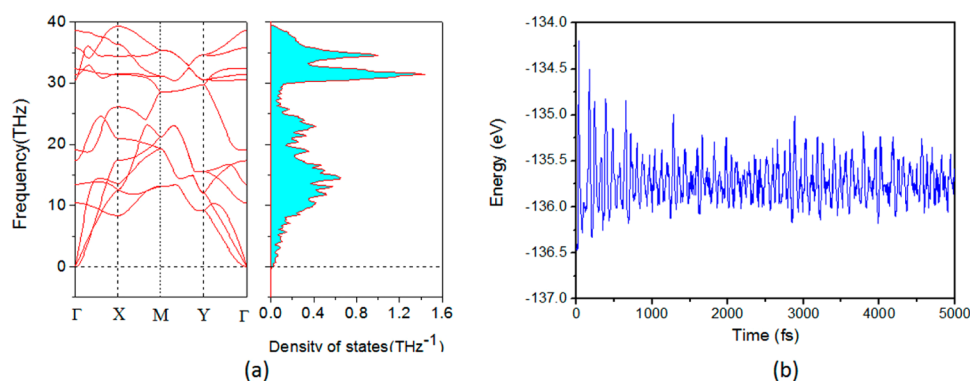


Figure 3. (a) Phonon dispersion band structures and the corresponding phonon density of states of the z-GMO. The high symmetric Brillouin zone points are Γ (0, 0, 0), X ($1/2$, 0, 0), M ($1/2$, $1/2$, 0), and Y (0, $1/2$, 0). (b) Energy fluctuation with respect to time in molecular dynamics simulations at 300 K.

value of total energy remains nearly constant during the simulation. After 5000 steps, the atomic structure is well sustained. When the temperature was further increased to 2000 K, we find that the structure can still remain intact without obvious distortion and it can be relaxed back to its original geometry when temperature was gradually reduced to 0 K. However, both ep- and mix-GMO dissociate into CO molecules when heated up to 2000 K. Similar calculations have also been carried out for the a-GMO structure (Figure S1–S3 of the Supporting Information) and found that the a-GMO structure is also dynamically stable and can stand temperatures as high as 2000 K. These results demonstrate that the z-GMO configuration we proposed in the present study is dynamically stable and is energetically much more stable than the previously reported ep-GMO and mix-GMO structures.

Although the stability of z-GMO has been confirmed, the feasibility of synthesis remains an issue. One may wonder: is it possible to synthesize z-GMO? Here, we propose a possible precursor for the structure as shown in Figure 4. In the initial geometry with a graphene-like hexagonal lattice, oxygen atoms reside on the hollow sites and the bridge sites. When fully optimized, this structure changes to z-GMO configuration without any energy barriers. This suggests that it is possible to synthesize the z-GMO in experiment.

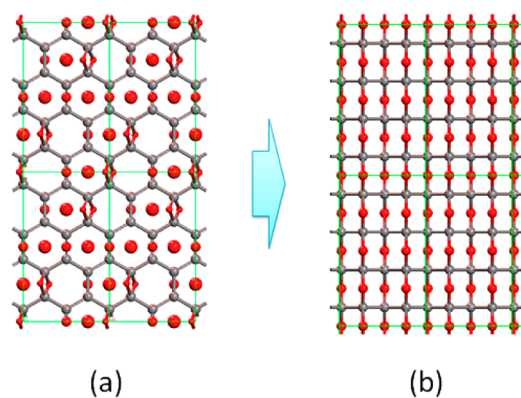


Figure 4. (a) Initial structure of the z-GMO precursor, (b) the optimized structure with z-GMO geometry. In the initial structure, the oxygen atoms in epoxy pair, normal epoxy and at hollow-site are represented by small, medium, and big red (dark gray) balls, respectively. Carbon atoms are represented by gray balls.

2. Properties. We, then, systematically studied the mechanical and electronic properties of the z-GMO. Graphene is well-known for its extremely high in-plane stiffness,¹⁶ and previous studies have demonstrated that upon oxidation the in-plane stiffness of graphene will be impaired.¹⁴ We hence investigated the elastic property of z-GMO structure to study the effect of oxidation on the mechanical properties. The in-plane uniaxial tensile modulus Y (Young's Modulus) is defined as

$$Y = \frac{1}{A} \left(\frac{\partial^2 E}{\partial \varepsilon^2} \right) \Bigg|_{\varepsilon=0}$$

where E is the total energy of the system in one unit cell with uniaxial strain ε , and A the equilibrium surface area of the unit cell. The variations of total energy with respect to the uniaxial strain along the x and y directions are plotted in parts a and b of Figure 5, respectively. The calculated uniaxial elastic modulus of

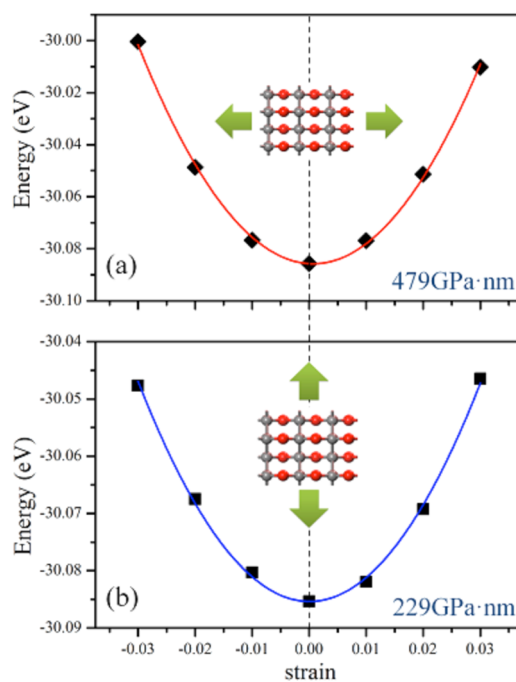


Figure 5. Energy changes with uniaxial strain along (a) ether and (b) zigzag C chain directions of z-GMO.

z-GMO along the x (Y_1) and y (Y_2) directions are found to be 479 GPa·nm and 229 GPa·nm, respectively, whereas the corresponding values of pristine graphene sheet are calculated to be 345 GPa·nm for both the zigzag and armchair directions in consistency with previous theoretical¹⁷ and experimental values.¹⁹ We see that the in-plane stiffness of the z-GMO is highly enhanced along the x direction, whereas it is greatly weakened along the y direction. Compared with the isotropic mechanical properties of the conventional pristine graphene sheet and its hydrogenated or fluorinated structures,¹⁸ the anisotropic elastic property exhibited in z-GMO is quite unique. The displayed directional anisotropy in z-GMO is due to the difference in strength between the O-bridged ether-type configuration and the zigzag C chains (in each unit cell, there are four C–O bonds in the x direction while only two C–C bonds exist in the y direction).

To understand the electronic properties of the z-GMO system, we calculated the band structure and corresponding partial density of states (PDOS). These are shown in parts a and b of Figure 6, respectively. No spin polarization is found,

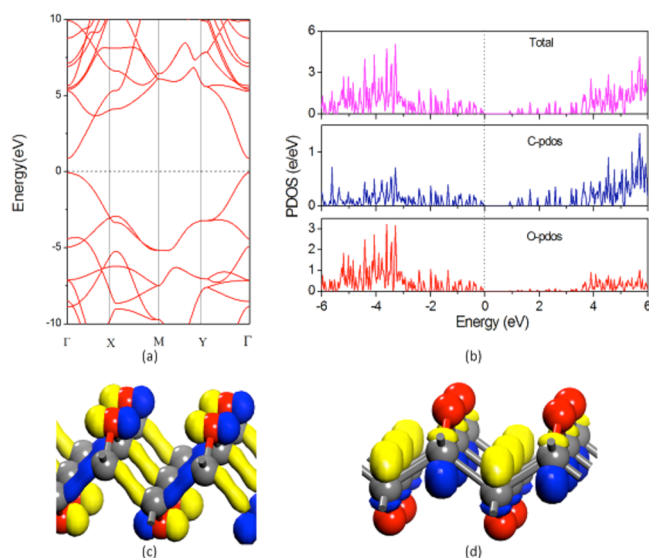


Figure 6. (a) Electronic band structure and (b) PDOS of the z-GMO. The Fermi energy level is shifted to 0 eV. (c) VBM and (d) CBM orbitals of z-GMO at the Γ point.

indicating that z-GMO is nonmagnetic. The band structure clearly shows that the z-GMO is a semiconductor with a direct band gap of 0.90 eV. This value is the same as that of the ep-GMO,⁷ suggesting that electronic band gap based experimental techniques are unable to distinguish the geometries of z-GMO and ep-GMO. The valence band maximum (VBM) and conduction band minimum (CBM) are both located at the Γ point of the Brillouin zone (Figure 6). The transition from metallic graphene to semiconducting z-GMO is due to the breakage of conjugated π network after oxidation. A careful examination of the bands near the Fermi level and the PDOS show that the VBM is contributed mainly by O p_y and C p_y orbitals, while the CBM mainly comes from the C p_z orbital. The VBM and CBM wave functions are plotted in parts c and d of Figure 6 showing that the VBM wave functions are localized on the O atoms and the C–C bonds, whereas the CBM wave functions are mainly contributed by the sp^3 antibonding orbitals of hybridized C atoms.

We next calculated the effective mass (m^*) of electron and hole in the valence and conduction bands of the z-GMO at the Γ point along the x (Γ -X) and the y (Γ -Y) directions. Unlike fluorinated monolayer and bilayer graphene which show isotropy in effective mass,¹⁹ our system exhibits distinct anisotropy. The magnitudes of effective masses of electrons and holes along the x direction are calculated to be $0.41 m_0$ and $2.11 m_0$ (where m_0 is the static mass of one electron), respectively, which are larger than those in the y direction ($0.21 m_0$ and $0.33 m_0$, respectively). This is because the band dispersion stems from the unique atomic arrangements, namely, the –C–O–C– configuration in the x direction and the –C–C–C– configuration in the y direction. The magnitudes of effective mass are comparable with those of zinc-blende GaN²⁰ suggesting that z-GMO can be used for electronic transport with significant anisotropic behaviors.

We further calculated the intrinsic electron (n) and hole (p) carrier concentration of the z-GMO structure. The electron and hole concentration n and p can be expressed as:

$$n = \int_{E_F}^{+\infty} D(E)f(E)dE$$

$$p = \int_{-\infty}^{E_F} D(E)[1 - f(E)]dE$$

where E_F is the Fermi energy, $D(E)$ is the total DOS, and $f(E)$ is the Fermi-Dirac distribution function. Intrinsic excitation requires the relationship of $n = p$. At room temperature, the calculated intrinsic carrier concentration is $\sim 7400 \text{ cm}^{-2}$.

3. Modulations. To modulate the physical properties such as band gap, effective mass, and carrier concentration, we used two strategies: strain engineering and full oxidation. We first apply biaxial strains to the z-GMO and examine the change of its geometry under strain. We find that the geometric structure can be retained below 10% compressive or tensile strain. As shown in part a of Figure 7, the band gap is greatly increased (decreased) under biaxial compression (tension) and changes from the equilibrium value of 0.90 to 2.41 eV under 10% compression. On the contrary, the band gap decreases monotonically to less than 0.01 eV when the tensile strain reaches to 10%. We note that, when tensile strain is further increased to 12%, the C–O bond of the z-GMO breaks. The main reason for the reduction of the band gap is that the C–O bond length increases under tension reducing the effect of O on the electronic structure. Thus, z-GMO behaves more like graphene, and accordingly, the band gap decreases. While under compression, the C–O bond length decreases which enhances the effect of O. Therefore, the system exhibits more features of oxide, and accordingly, the band gap increases. The large variation in the band gap illustrates the flexibility of strain in tuning the electronic and transport properties z-GMO.

The effect of biaxial strain on the effective mass of the z-GMO is also studied. The variations of effective mass of the valence and conduction bands along the x (Γ -X) ($m_{v,x}^*$ and $m_{c,x}^*$) and the y (Γ -Y) directions ($m_{v,y}^*$ and $m_{c,y}^*$) with respect to the biaxial strains are plotted in part b of Figure 7, respectively. We see that the magnitude of $m_{v,x}^*$ is more sensitive to strain as compared to $m_{v,y}^*$, $m_{c,x}^*$ and $m_{c,y}^*$. This can be understood from the VBM orbital distribution in part c of Figure 6 where the O bonding dominates the VBM and the strain can easily enhance or reduce the effect of oxidation. In part c of Figure 7, we plot the carrier concentration (N , in log form) variation with respect to the biaxial strain and

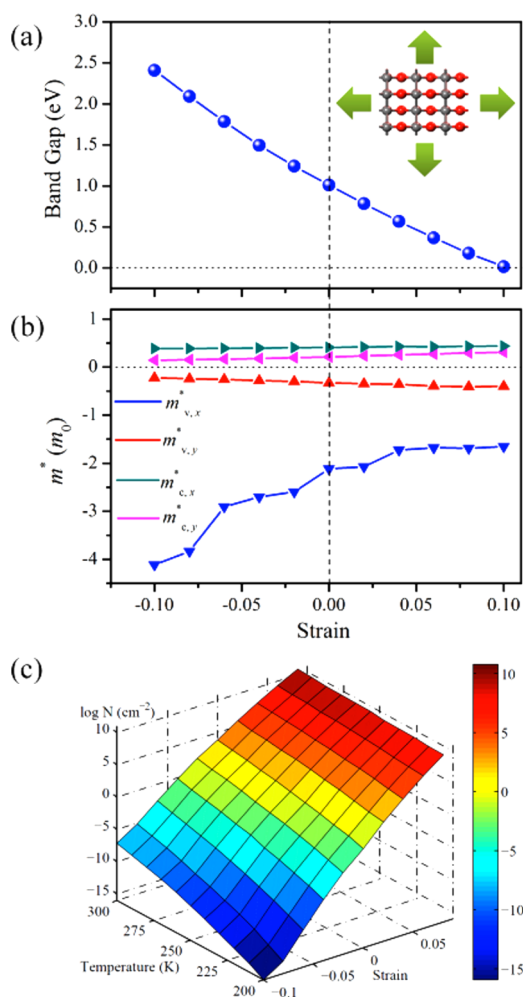


Figure 7. Changes of the band gap (a), effective mass (b), and carrier concentration (c) of z-GMO with the biaxial strains.

environmental temperature. It can be seen that the carrier concentration increases almost exponentially when tensile strain is applied. This is due to the reduction of band gap under tension resulting in more electrons thermally excited to the conduction bands. At room temperature, the carrier concentration can be increased (decreased) to $\sim 10^{11}$ cm^{-2} (10^{-5} cm^{-2}) under tensile (compressive) strain from $\sim 10^4$ cm^{-2} in the free state. Thus far, we have demonstrated that strain can effectively modify the electronic properties of z-GMO.

Next, we explore another possible way to tune the properties of z-GMO by using oxidation with higher concentration. On the basis of our finding that z-GMO with ether type configuration has lower energy, we propose a geometry for the fully oxidized graphene sheet with a C:O ratio of 1:2 (graphene dioxide, GDO), and find that the properties change significantly. In the GDO, as shown in Figure 8, all of the C–C bonds are broken by oxidation. Molecular dynamics simulation indicates that this phase is also thermodynamically stable at room temperature, but it dissociates into CO_2 molecules when temperature reaches 500 K. Electronic structure calculations show (Figure 9) that the GDO is an indirect band gap insulator with a large gap of 3.90 eV. The VBM is located at the X point in the Brillouin Zone while the CBM is located at the Γ point. This is quite different from that of the z-GMO, which is a direct gap semiconductor with a small gap of 0.9 eV. The PDOS

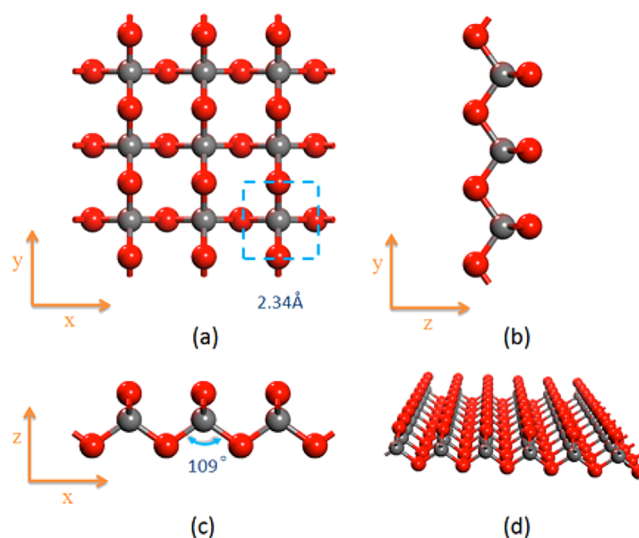


Figure 8. Different views of the geometry of GDO.

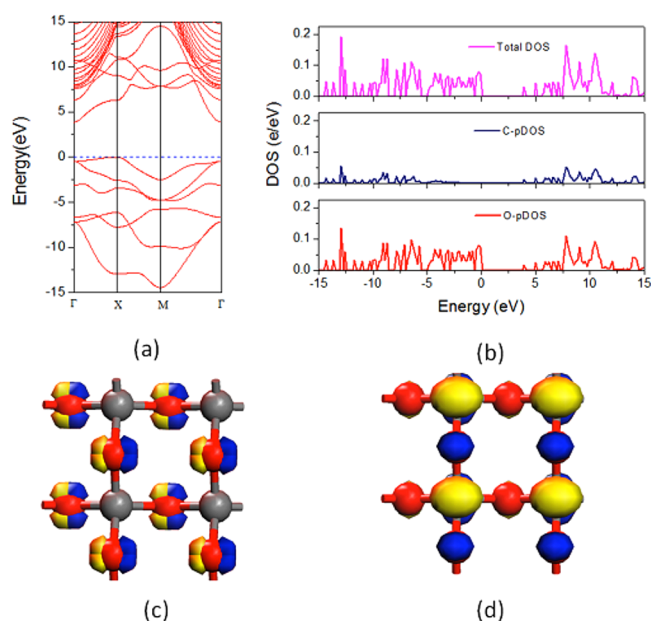


Figure 9. (a) Electronic band structure, (b) PDOS, (c) VBM (Γ point), and (d) CBM (X point) orbitals of the GDO.

shows that the VBM is mainly contributed by $2p$ electrons of the O, whereas the CBM originates from the $2p$ orbitals of both O and C, which are also different from the orbital distributions of z-GMO. The underlying reasons for these differences are due to the different bonding features in the two systems. In the GDO, the O–C–O bonding angle is 109° having perfect sp^3 hybridizations. The resulting σ bonding lies deep below the Fermi energy while the σ^* antibonding lies high in energy above the Fermi level. Additionally, due to its higher symmetry in geometry, the in-plane elastic modulus of GDO exhibits isotropy in x and y direction (Table 1). Therefore, we demonstrate that oxidation is an effective way to functionalize graphene and tune the physical properties of graphene-based materials.

The dynamic stability of GMO is studied by carrying out molecular dynamics simulations at $T = 300$ and 500 K. An 8×8 supercell containing 192 atoms is used in simulation in order to reduce the constraint imposed by lattice periodicity. We find

Table 1. Comparison of in-Plane Elastic Modulus (Y_1 , Y_2), Energy Band Gap and Temperature at Which the Structures Remain Stable for All the Studied Systems

structure	Y_1 (GPa·nm)	Y_2 (GPa·nm)	band gap (eV)	T (K)
graphene	345	345	0.0	>2600 (ref 21)
z-GMO	479	226	0.9	2000
a-GMO	514	188	3.9	2000
ep-GMO	282	208	0.9 (ref ⁷)	1000
mix-GMO	153	201	4.0	1500
GDO	336	336	3.9	300

that GDO can be stable at 300 K but not at 500 K (Figure 10). This differs from GMO, which was observed to be stable even at 2000 K. Therefore, GDO is thermodynamically less stable as compared to GMO. Because GDO has a high oxidation level (C:O = 1:2), the fabrication using conventional methods might encounter some difficulties. We noticed that the GDO structure we proposed here is identical to a single layer of the layered polymeric CO₂ in high pressure phase.^{2,3}

IV. SUMMARY

We have carried out comprehensive studies on geometry, stability, in-plane elastic modulus, effective mass, and carrier concentration of stoichiometric graphene oxide. The main results are summarized in Table 1, from which the following conclusions can be drawn: (1) We have found a new ether-type structure of GMO (z-GMO), which consists of zigzag carbon chains linked by O atoms and is much more stable than both the ep-GMO^{7,8} and the mix-GMO⁸ configurations suggested earlier. This enhanced stability is due to the reduction in strain by changing the epoxy-pair type configuration to ether-type one. (2) The z-GMO has anisotropic mechanical and electronic transport properties which are quite different from the conventional 2D nanomaterials such as graphene, BN, and their hydrogenated (fluorinated) systems. (3) The band gap, effective mass, and intrinsic carrier concentration of z-GMO

can be effectively modulated by applying biaxial strain. (4) Compared with the z-GMO, the GDO consists of –C–O–C–O–C– zigzag chains in both the x and y directions, the anisotropies of carrier transportation and mechanical modulus displayed in the z-GMO do not exist in the GDO anymore (Table 1) indicating that oxidation level can manipulate anisotropy in graphene oxide. In addition, we further show that z-GMO can be used as a substrate for single layer deposition of metal atoms (Supporting Information). It should be mentioned that the GGA calculations would underestimate the band gap. Using hybrid HSE06 functional,²² we found that the band gap changes to 3.21 and 6.87 eV for GMO and GDO, respectively. However, our main task in this study is for the thermal and dynamical stabilities of GMO and GDO. So our main conclusions remain unchanged.

From graphene to GMO and to GDO, the C–C bonds are gradually broken by oxidation, the bonding of C atoms goes from sp^2 to distorted sp^3 and to perfect sp^3 , and the resulting electronic structure and mechanical properties are changed dramatically as a result. Graphene and graphene dioxide are two extreme cases in the graphene oxide family with GMO being one of the specific in-between states. Therefore, an in-depth study of GMO and GDO is of special significance for understanding and exploring graphene oxide based materials. We hope that our efforts would stimulate further research in this hotly pursued field.

■ ASSOCIATED CONTENT

Supporting Information

Structural parameters of all of the studied structures; geometric structure, stability, and electronic properties of a-GMO configuration; single layer deposition of metal atoms on z-GMO. This material is available free of charge via the Internet at <http://pubs.acs.org>.

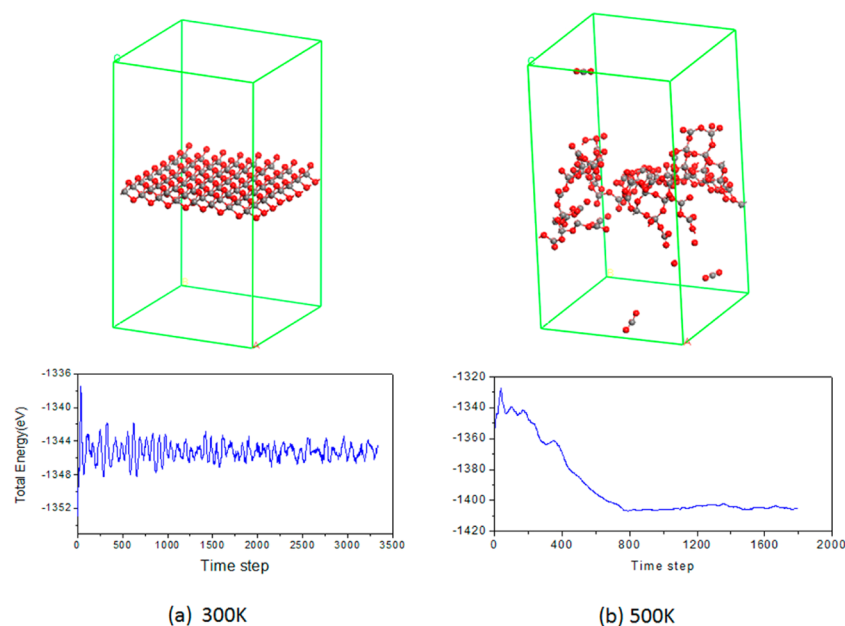


Figure 10. Upper panel: snapshots of the atomic configuration of GDO of molecular simulation for $T = 300$ K (a) and 500 K (b). Lower panel: total energy fluctuation with respect to time.

AUTHOR INFORMATION

Corresponding Author

*E-mail: qianwang2@pku.edu.cn.

Notes

The authors declare no competing financial interest.

ACKNOWLEDGMENTS

This work is supported by grants from the National Natural Science Foundation of China (Grant Nos. NSFC-11174014 and NSFC-21273012), the National Grand Fundamental Research 973 Program of China (Grant No. 2012CB921404), and from the U.S. Department of Energy. The computational resources utilized in this research was provided by Shanghai Supercomputer Center.

REFERENCES

- (1) Novoselov, K. S.; Geim, A. K.; Morozov, S. V.; Jiang, D.; Zhang, Y.; Dubonos, S. V.; Grigorieva, I.; Filrsov, A. A. *Science* **2004**, *306*, 666.
- (2) Geim, A. K.; Novoselov, K. S. *Nat. Mater.* **2007**, *6*, 183.
- (3) Lerf, A.; Heb, H.; Riedl, T.; Forster, M.; Klinowskib, J. *Solid State Ionics* **1997**, *857*, 101.
- (4) He, H.; Klinowski, J.; Forster, M.; Lerf, A. *Chem. Phys. Lett.* **1998**, *287*, 53.
- (5) Mkhoyan, K. A.; Contryman, A. W.; Silcox, J.; Stewart, D. A.; Eda, G.; Mattevi, C.; Miller, S.; Chhowalla, M. *Nano Lett.* **2009**, *9*, 1058.
- (6) Szabó, T.; Berkesi, O.; Forgó, P.; Josepovits, K.; Sanakis, Y.; Petridis, D.; Dékány, I. *Chem. Mater.* **2006**, *18*, 2740.
- (7) Mattson, E. C.; Pu, H.; Cui, S.; Schofield, M. A.; Rhim, S.; Lu, G.; Nasse, M. J.; Ruoff, R. S.; Weinert, M.; Gajdardziska-Josifovska, M.; Chen, J. H.; Hirschmugl, C. J. *ACS Nano* **2011**, *5*, 9710.
- (8) Xiang, H. J.; Wei, S.-H.; Gong, X. G. *Phys. Rev. B* **2010**, *82*, 035416.
- (9) Blöchl, P. E. *Phys. Rev. B* **1994**, *50*, 17953.
- (10) Kresse, G.; Furthmüller, J. *Phys. Rev. B* **1996**, *54*, 11169.
- (11) Perdew, J. P.; Burke, K.; Ernzerhof, M. *Phys. Rev. Lett.* **1996**, *77*, 3865.
- (12) Monkhorst, H. J.; Pack, J. D. *Phys. Rev. B* **1976**, *13*, 5188.
- (13) Togo, A.; Oba, F.; Tanaka, I. *Phys. Rev. B* **2008**, *78*, 134106.
- (14) Lahaye, R. J. W. E.; Jeong, H. K.; Park, C. Y.; Lee, Y. H. *Phys. Rev. B* **2009**, *79*, 125435.
- (15) Nosé, S. J. *Chem. Phys.* **1984**, *81*, 511.
- (16) Lee, C.; Wei, X.; Kysar, J. W.; Hone, J. *Science* **2008**, *321*, 385.
- (17) Liu, F.; Ming, P.; Li, J. *Phys. Rev. B* **2007**, *76*, 064120.
- (18) Sahin, H.; Topsakal, M.; Ciraci, S. *Phys. Rev. B* **2011**, *83*, 115432.
- (19) Sivek, J.; Leenaerts, O.; Partoens, B.; Peeters, F. M. J. *Phys. Chem. C* **2012**, *116*, 19240.
- (20) Yu, P. Y.; Cardona, M. *Fundamentals of Semiconductors: Physics and Materials properties*, 3rd ed.; Springer: Berlin, Heidelberg, 2005.
- (21) Kim, K.; Regan, W.; Geng, B.; Alemán, B.; Kessler, B. M.; Wang, F.; Crommie, M. F.; Zettl, A. *Phys. Status Solidi RRL* **2010**, *4*, 302.
- (22) Heyd, J.; Scuseria, G. E.; Ernzerhof, M. J. *Chem. Phys.* **2003**, *118*, 8207.
- (23) Sun, J.; Klug, D. D.; Martonak, R.; Montoyad, J. A.; Leef, M. S.; Scandolo, S.o; Tosattid, E. *Proc. Natl. Acad. Sci. U.S.A.* **2009**, *106*, 6077.